Nanoscale

PAPER

View Article Online
View Journal | View Issue

Cite this: *Nanoscale*, 2015, **7**, 12659

Water–methanol separation with carbon nanotubes and electric fields†

Winarto, Daisuke Takaiwa, Eiji Yamamoto and Kenji Yasuoka*

Received 6th April 2015,
Accepted 17th June 2015

DOI: 10.1039/c5nr02182k

www.rsc.org/nanoscale

Methanol is used in various applications, such as fuel for transportation vehicles, fuel cells, and in chemical industrial processes. Conventionally, separation of methanol from aqueous solution is by distillation. However, this method consumes a large amount of energy; hence development of a new method is needed. In this work, molecular dynamics simulations are performed to investigate the effect of an electric field on water–methanol separation by carbon nanotubes (CNTs) with diameters of 0.81 to 4.07 nm. Without an electric field, methanol molecules fill the CNTs in preference to water molecules. The preference of methanol to occupy the CNTs over water results in a separation effect. This separation effect is strong for small CNT diameters and significantly decreases with increasing diameter. In contrast, under an electric field, water molecules strongly prefer to occupy the CNTs over methanol molecules, resulting in a separation effect for water. More interestingly, the separation effect for water does not decrease with increasing CNT diameter. Formation of water structures in CNTs induced by an electric field has an important role in the separation of water from methanol.

1. Introduction

Methanol is used as an alternative energy resource to reduce the use of fossil fuels.[1–3] Methanol blended with gasoline improves the thermal efficiency of engines and reduces the emission of exhaust gas.[4–7] Another application of methanol is in fuel cells to directly convert chemical energy to electric energy, and offers clean energy conversion.[8–11] In addition, methanol is important in chemical industrial processes.[12]

As renewable energy, methanol can be produced by fermentation of biomass, such as corn, sugarcane, sorghum, and microalgae.[13–16] In the production processes, separation of methanol from aqueous solution is required. Conventionally, methanol is separated from aqueous solution by distillation, but this process consumes large amounts of energy.[17,18] Some alternative methods have been developed and applied, such as pervaporation,[19–21] adsorption to zeolite,[22–24] gas stripping,[25] using ionic liquids,[26,27] and filtering with nanotubes.[28] However, it is still a challenge to develop an innovative technique to more effectively separate methanol from aqueous solution.

In the recent years, carbon nanotubes (CNTs) have shown promise as separation membranes for gas,[29,30] desalination,[31–33] gas–water,[34] and organics–water separation.[35] Moreover, the study of the separation of methanol from aqueous solution with CNTs has attracted considerable attention. Under a chemically potential gradient, methanol molecules flow through CNTs in preference to water molecules.[36] Modification of CNT hydrophobicity by attaching carboxyl acid (COOH) groups on the inner wall of the CNTs slightly increases the selectivity of methanol molecules over water molecules.[36] When CNTs are immersed in water–methanol solution, methanol molecules preferentially fill and occupy the CNTs over water molecules, resulting in a separation effect.[37] However, the selectivity significantly decreases with increasing CNT diameter.[37] Immersing CNTs in methanol and other alcohol solutions shows that the selectivity for alcohols over water in occupying CNTs also depends on the number of alcohol–carbon atoms.[38]

Water confined in nanoscale space under an electric field has many interesting properties, which is very important for nanotechnology and biological science. A significant number of studies concerned with the effects of an electric field of the order up to 8 V nm^{-1} on water confined in CNTs and between two-plates were reported recently.[39–46] The strength of that field is still comparable with the typical field in biological transmembrane channels, which is 0.06 to 0.3 V nm^{-1}.[47,48] Moreover, various strategies to explore the field effects for developing nanofluidic devices have been reported as well. Nanopumping can be performed by employing a time-

Department of Mechanical Engineering, Keio University, 3-14-1 Hiyoshi, Kohoku-ku, Yokohama 223-8522, Japan. Fax: +81-45-566-1495; Tel: +81-45-566-1523; E-mail: yasuoka@mech.keio.ac.jp

†Electronic supplementary information (ESI) available: Molecule structures in carbon nanotubes. Water molecules *vs.* methanol molecules in carbon nanotubes under electric field. See DOI: 10.1039/c5nr02182k

dependent, vibration, and rotating electric field.[49–52] Introducing an electric field along the CNT can enhance reverse osmosis for water purification.[53] The axial field can control the dynamics of water molecules in the CNT to induce flow.[54]

In this work, we investigated the separation of water and methanol from water–methanol solutions with CNTs with and without an axial electric field using molecular dynamics (MD) simulations. We investigate the effect of an electric field on the selectivity of a water–methanol mixture flowing into (6, 6) to (30, 30) CNTs. In the absence of an electric field, methanol molecules preferentially enter and occupy the CNTs over water molecules, resulting in a separation effect for methanol. However, the separation effect for methanol is only strong for small CNT diameter and considerably decreases with increasing CNT diameter. In contrast, when an electric field is applied, water molecules strongly prefer to enter and occupy the CNTs over methanol molecules, which produce a separation effect for water. More importantly, the selectivity for water molecules does not depend on the CNT diameter, indicating a strong separation effect for water.

2. Methods

Similar to our previous study,[55] the simulation system consisted of a CNT, two graphene sheets, and water–methanol reservoirs on both sides (Fig. 1A and B), which differs from other studies.[37,38] In the simulation system, the length of the CNT was 2.95 nm with various diameters: 0.81, 0.95, 1.08, 1.22, 1.36, 1.63, 2.03, 2.71, 3.39, and 4.07 nm for (6, 6), (7, 7), (8, 8), (9, 9), (10, 10), (12, 12), (15, 15), (20, 20), (25, 25), and (30, 30) CNTs, respectively. The reservoirs were filled with a mixture of water and methanol molecules. In the reservoirs, we considered mole fractions of water molecules (χ_{water}) of 0.81 and 0.19, which are equivalent to 70% and 12% mass fractions, respectively. Periodic boundary conditions were applied in all directions (x, y, and z axes).

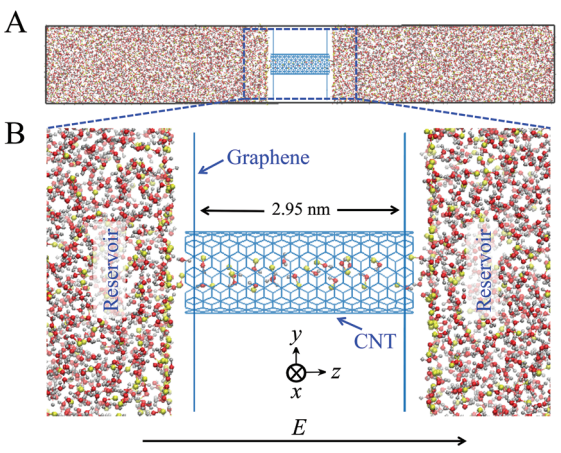

Fig. 1 (A) Molecular dynamics (MD) simulation system consisting of two graphene sheets, a CNT, and reservoirs filled with a water–methanol mixture. (B) Magnified image of the MD system. A homogeneous electric field $\boldsymbol{E}$ was applied in the z axis direction.

The SPC model[56] was used for water and the OPLS united-atom potentials[57,58] were used for methanol. The OPLS united-atom force field has been widely used for molecular simulation studies.[36,37,59] The Lennard-Jones (LJ) parameters are σ_O = 0.3166 nm and ε_O = 0.6500 kJ mol^{-1} for the oxygen of water, σ_C = 0.3400 nm and ε_C = 0.3612 kJ mol^{-1} for carbon of the CNT, σ_O = 0.3070 nm and ε_O = 0.7113 kJ mol^{-1} for the oxygen of methanol, and σ_{CH_3} = 0.3775 nm and ε_{CH_3} = 0.8661 kJ mol^{-1} for CH_3 (methyl). The LJ parameters for determining the interactions between different atoms were calculated with the combination rule $\sigma_{ij} = (\sigma_i\sigma_j)^{1/2}$ and $\varepsilon_{ij} = (\varepsilon_i\varepsilon_j)^{1/2}$. A homogeneous electric field of up to $\boldsymbol{E}$ = 2 V nm^{-1} was applied in the direction of the positive z axis. Here, the magnitude of the electric field was still lower than the threshold value of $\boldsymbol{E}$ = 3.5 V nm^{-1} where dissociation of water molecules occurs,[60] and within the range of an experimental study of graphene.[61]

The MD simulations were carried out using GROMACS 4.5.5 software.[62] The van der Waals interactions were cut off at 1.5 nm, and electrostatic interactions were treated using the particle mesh Ewald method[63] with the real space cutoff set to 1.5 nm. The length of the chemical bonds of the water and methanol molecules and the angles between the bonds were kept constant with the SHAKE algorithm.[64] The CNTs and graphene were made rigid by fixing the lengths and angles of the chemical bonds. The simulations were performed with $NL_x\,L_y\,P_z\,T$, where the temperature (T) was maintained at 300 K with the Nosé–Hoover coupling scheme.[65,66] The pressure in the axial direction (z axis) was maintained at 0.1 MPa using the Parrinello–Rahman technique.[67] The time step was set to 2 fs and the simulations were run for a minimum of 25 ns, where the systems reached an equilibrium state at around 2 ns.

3. Results and discussion

To determine the preferential occupancy of molecules in the CNTs, we calculated the mole fractions in the CNTs and compared them with those in the reservoirs, as shown in Fig. 2. With no electric field (*i.e.*, $\boldsymbol{E}$ = 0 V nm^{-1}), χ_{water} in the CNTs is lower (or $\chi_{methanol}$ in the CNTs is higher) than that in the reservoirs for both χ_{water} = 0.81 and 0.19 (black dotted lines), as shown in Fig. 2A and B, respectively. The preference for methanol molecules to occupy the CNTs over water molecules produces a separation effect for methanol. This separation effect is strong for the (6, 6) CNT. However, it significantly decreases with increasing CNT diameter, confirming the results of a previous study.[37]

In contrast, with an electric field, water molecules occupy the CNTs in preference to methanol molecules. With $\boldsymbol{E}$ = 0.25 V nm^{-1}, χ_{water} in the CNTs increases with increasing CNT diameter. With the stronger electric fields of $\boldsymbol{E}$ = 1 V nm^{-1} and 2 V nm^{-1}, χ_{water} = 1.0 for all CNT diameters (Fig. 2A). In Fig. 2B, even though χ_{water} in the reservoirs is very low (0.19), χ_{water} = 1.0 in the CNTs with 2 V nm^{-1} for (6, 6) to (15, 15) CNTs. For

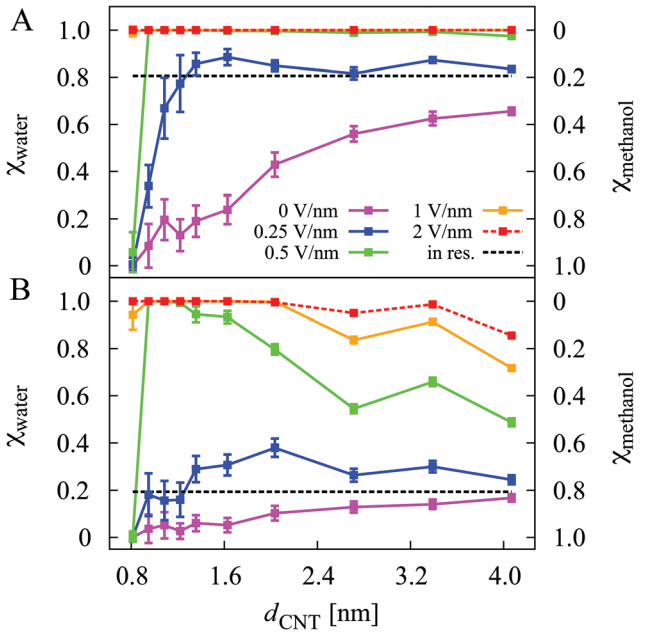

Fig. 2 Mole fraction inside CNTs in the diameter range 0.81–4.07 nm with E = 0, 0.25, 0.5, 1, and 2 V nm^{-1}. The left vertical axis shows the mole fraction of water molecules (χ_{water}) and the right axis shows the mole fraction of methanol molecules ($\chi_{methanol}$). (A) χ_{water} = 0.81 (black dotted line) in the reservoirs and (B) χ_{water} = 0.19 (black dotted line) in the reservoirs. The error bars represent the standard deviation.

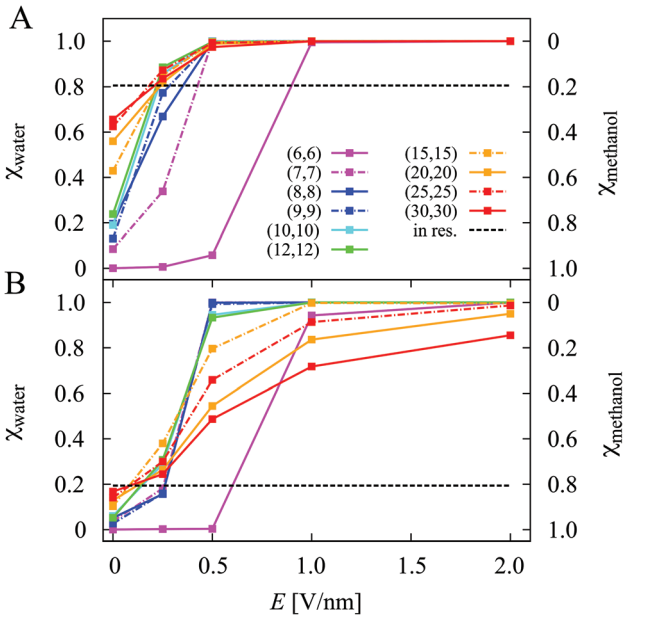

Fig. 3 Dependency of χ_{water} (or $\chi_{methanol}$) on the electric field strength (E) in (6, 6)–(30, 30) CNTs. (A) χ_{water} = 0.81 (black dotted line) in the reservoirs. (B) χ_{water} = 0.19 (black dotted line) in the reservoirs.

the larger CNT diameters, it slightly decreases to 0.95, 0.99, and 0.86 for (20, 20), (25, 25), and (30, 30) CNTs, respectively. These results indicate that an electric field makes the preference for water molecules in the CNTs very strong. As a result, it produces a strong separation effect for water. Moreover, the separation effect for water is strong for a wide range of CNT diameters. This is advantageous because practical synthesis of CNTs results in various diameters, and not uniformly small CNTs.[68–70]

The separation effect for water in the CNTs is clear by plotting χ_{water} against E, as shown in Fig. 3. With E = 0.25 V nm^{-1}, the electric field effect is observed, where χ_{water} in the CNTs is high, except for CNT (6, 6). For E = 0.5 V nm^{-1}, χ_{water} = 1.0 in (7, 7) to (30, 30) CNTs, but in the (6, 6) CNT it is still very low (Fig. 3A). Similarly, for χ_{water} = 0.19 in the reservoir and E = 0.5 V nm^{-1}, χ_{water} is high in all of the CNTs, except for the (6, 6) CNT (Fig. 3B). The electric field effect in the (6, 6) CNT is strong for $E \geq 1$ V nm^{-1}. The results in Fig. 3 show that for $E \leq$ 0.5 V nm^{-1} the electric field effect on water–methanol separation in the (6, 6) CNT is weaker than that in the other CNTs. Methanol molecules in the (6, 6) CNT are more stable than water molecules, as seen in the case with no electric field. This strongly depends on the water molecule structure in the CNTs, which will be discussed in the following paragraph.

Fig. 4 shows snapshots of the structures of molecules in the (8, 8) CNT with E = 0, 0.25, 0.5, and 2 V nm^{-1}. With E = 0 and 0.25 V nm^{-1}, both water and methanol molecules occupy the CNTs. With stronger electric fields (E = 0.5 and 2 V nm^{-1}), only

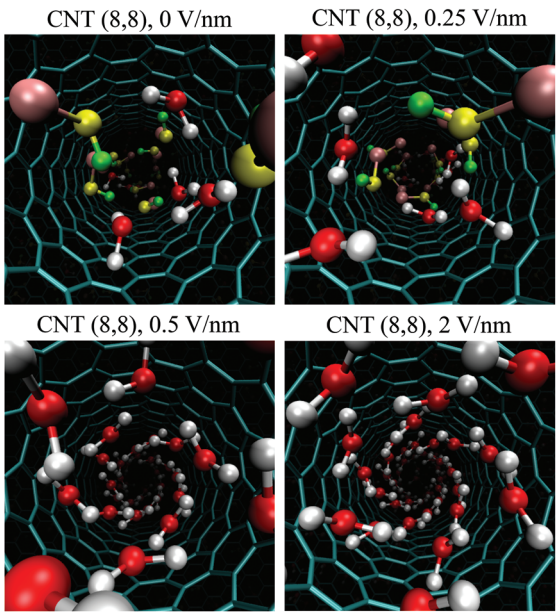

Fig. 4 Structures of molecules in the (8, 8) CNT with E = 0, 0.25, 0.5, and 2 V nm^{-1}. Red and white atoms denote water molecules. Methanol molecules are represented by yellow, green, and pink for oxygen, hydrogen, and methyl, respectively. χ_{water} = 0.81 in the reservoirs.

water molecules occupy the CNT. Interestingly, the water molecules form helical structures, which are ordered solid-like structures. These structures are ice-nanotube structures induced by the electric fields.[40,42–44,55] As previously reported, the dipole moments of water molecules align parallel to the

electric field, increasing the density of water molecules in the CNTs and inducing the formation of ordered solid-like structures.[39,55] Although the water molecules form solid-like structures in the CNTs, permeation analysis showed that they can flow like liquid.[55] The formation of ordered structures induced by an electric field plays an important role in the separation of water–methanol solution. The ordered structures can be helical or non-helical depending on the CNT diameter and strength of the electric field. As an example, the structure in (10, 10) CNT with 1 V nm^{-1} is helical, and with 2 V nm^{-1} it is not helical where the structure index is $n = m$.[55] Snapshots of structures in (7, 7) to (30, 30) CNTs with 2 V nm^{-1} are shown in Fig. S1 (see the ESI†).

To investigate the formation of the ordered structures, we calculated the radial density distributions of the atoms in the CNTs. For the (8, 8) CNT with $\boldsymbol{E}$ = 0.25 V nm^{-1}, χ_{water} = 0.67 in the CNT (Fig. 5A and B). Water and methanol molecules are concentrated in a narrow region around the central axis of the CNT. The orthographic projection of the snapshot in Fig. 5B confirms the results. With no electric field, the radial density distribution shows the same tendency as E = 0.25 V nm^{-1}. For an electric field of $\boldsymbol{E} \geq$ 0.5 V nm^{-1}, the width of the peak of the distribution is narrower and the peak position shifts towards the CNT (see Fig. S2 and S3 in the ESI.†)

An electric field aligns the orientation of the water and methanol molecules. For the water molecules, because they have the same orientation and are close together, it is easy to form an ordered hydrogen bonded network. Unlike water molecules, methanol molecules are not symmetrical. Moreover, for bulk methanol, hydrogen bonds only form between the oxygen and hydrogen atoms, while it is difficult for the methyl groups to form hydrogen bonds.[71,72] Thus, methanol molecules in the CNTs cannot form an ordered hydrogen bonded network with all of their atoms, such as that formed by water molecules. The number of hydrogen bonds per methanol molecule in the methanol molecule structure is less than the number of hydrogen bonds per water molecule in the water molecule structure. In other words, the water molecule structures are more stable than the methanol molecule structures in CNTs under an electric field.

Two-dimensional (2D) structures of the molecules in the (8, 8) CNT for $\boldsymbol{E}$ = 0, 0.25, and 0.5 V nm^{-1} are shown in Fig. 6. All of the atoms in the CNT were radially projected on the tube surface, as shown in Fig. 5. The 2D structures were obtained by unrolling the tube. The directions of the dipole moments of both water and methanol molecules with $\boldsymbol{E}$ = 0.25 V nm^{-1} are more uniform than with no electric field. For $\boldsymbol{E}$ = 0.25 V nm^{-1}, it is noticeable that the water molecules begin to form a hydrogen bonded network, whereas methanol molecules form a linear hydrogen bonded structure where only the oxygen and hydrogen atoms form hydrogen bonds with neighboring molecules. The methyl groups do not contribute to the hydrogen bonded network. With $\boldsymbol{E}$ = 0.5 V nm^{-1}, the density of water molecules in the CNT increases compared with no electric field, and they form an ordered hydrogen bonded network with the (4, 2) ice structure.

Under an electric field and confined between the CNT walls, the water molecule structures in the CNTs are stable. Moreover, the electric field increases the density of water molecules in the CNTs compared with no electric field. This removes methanol molecules from the CNTs, and the methanol molecules cannot disrupt the water structures to permeate into the CNTs from the reservoirs. Confinement between the CNT walls is weaker with increasing CNT diameter. The

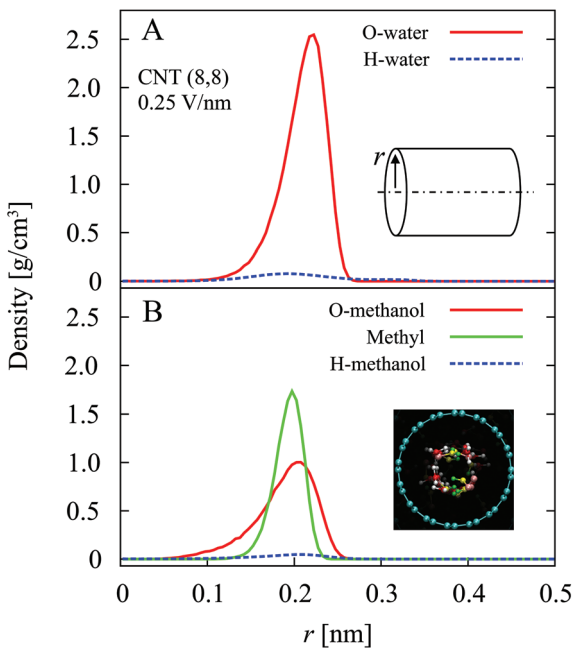

Fig. 5 Radial density distribution of atoms in the (8, 8) CNT with $\boldsymbol{E}$ = 0.25 V nm^{-1} and χ_{water} = 0.81 in the reservoirs for (A) water molecules, and (B) methanol molecules. O-water, H-water, O-methanol, and H-methanol indicate oxygen and hydrogen atoms of the water and methanol molecules. Only one hydrogen atom of every water molecule was considered for the calculation. Water and methanol molecules are concentrated in a narrow region in the radial direction, as confirmed by the snapshot in (B).

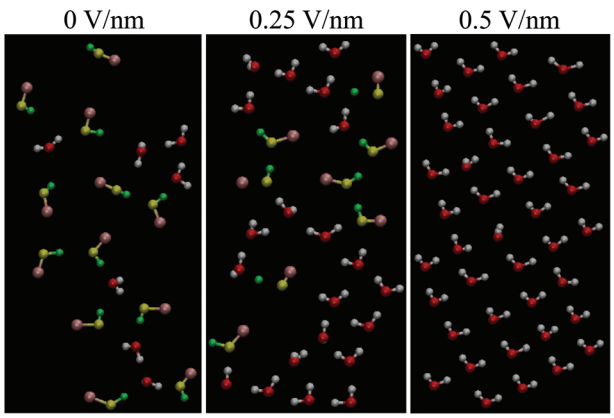

Fig. 6 Two-dimensional structures of molecules in the (8, 8) CNT for $\boldsymbol{E}$ = 0, 0.25 and 0.5 V nm^{-1}. χ_{water} = 0.81 in the reservoirs.

stability of the water structures decreases with increasing CNT diameter. As a result, the separation effect for water decreases with increasing CNT diameter (Fig. 2B).

Fig. 3 shows that the separation effect for water with an electric field of $\boldsymbol{E} \leq 0.5$ V nm^{-1} in the (6, 6) CNT is weaker than that in the larger CNTs. The water structure in a narrow CNT, such as CNT (6, 6), is a single-file structure.[73–75] This means that water molecules form a linear hydrogen bonded structure. Only one hydrogen atom of a water molecule forms a hydrogen bond with another water molecule. Thus, the maximum number of hydrogen bonds per water molecule is two. This differs from the water structures in the wider CNTs, where both hydrogen atoms of a water molecule can form hydrogen bonds with other molecules, making the water structures stable. As a result, the separation effect for water in the (6, 6) CNT with $\boldsymbol{E} \leq 0.5$ V nm^{-1} is weaker than that in the larger CNTs (Fig. 3). With $\boldsymbol{E} \geq 1$ V nm^{-1}, the water structure in the (6, 6) CNT is a zig-zag single-file structure (see Fig. S4 in the ESI†). As shown in Fig. S4,† for $\boldsymbol{E}$ = 0–0.5 V nm^{-1}, methanol molecules prefer to fill the (6, 6) CNT with single-file structures. For $\boldsymbol{E}$ = 1 V nm^{-1}, water molecules rather than methanol molecules occupy the CNT and form a zig-zag structure. The dipole moments of the water molecules are aligned parallel to the electric field with hydrogen bonds between water molecules, which makes the structure more stable than methanol molecule structures. With a stronger field of $\boldsymbol{E}$ = 2 V nm^{-1}, the density of water molecules in the CNT is higher than with weaker electric fields.

To clarify the separation process, we performed additional simulation by filling the reservoir with methanol molecules only (the system consisted of a CNT, graphene, and methanol). We investigated the effect of an electric field on the methanol molecules inside CNTs and compared with that on water molecules (see Fig. S5–S11 and Tables S1–S3 in the ESI† for more details). The electric field aligns the dipole moment of methanol molecules parallel to the field. As a result, the occupancy of methanol molecules in the CNTs increases even in a small (6, 6) CNT. Methanol molecules prefer to fill in the CNTs under the electric field. These results are the same as the effect of the field on water molecules. Difference of potential energy in the CNT (U_{CNT}) and in the reservoir (U_{res}), $\Delta U = U_{CNT} - U_{res}$, decreases with the field. That facilitates water and methanol molecules to fill the CNT. Thus, the potential energy analysis supports the notion that water and methanol molecules prefer to occupy the CNT under the electric field.

As shown in the previous study,[37] the van der Waals attraction for methanol–CNT is stronger than that for water–CNT. The attraction for methanol–CNT decreases slightly with an electric field. In contrast, with an electric field, van der Waals interaction between water and CNT becomes repulsive. This implies that preferential occupancy of water molecules in CNTs over methanol molecules is not due to the interaction of water–CNT. The result suggests that the hydrogen bond network in the water structure is a key factor for the separation effect with an electric field. Because methyl groups cannot form hydrogen bonds, the average number of hydrogen bonds per molecule for water is larger than that for methanol, which are 2.77 and 1.83 in (8, 8) CNT with 2 V nm^{-1}, respectively. Moreover, the water molecules structure consists of some line-structures that are hydrogen bonded to each other, such as a net structure. Meanwhile, the methanol molecules structure is composed of independent line-structures that are not hydrogen bonded to one another. As a result, the water structure in CNTs is more stable than the methanol structure. With 2 V nm^{-1}, ΔU of Coulomb potential energy per molecule for water is lower than that for methanol, which are −31.55 kJ mol^{-1} and −17.97 kJ mol^{-1}, respectively. These data imply that the electrostatic interaction in the water structure is stronger than that in the methanol structure.

The structure of water molecules confined in nanospace is strongly influenced by the orientation of the electric field. The axial field induces the formation of ordered structures, whereas a perpendicular electric field disrupts the hydrogen bond structure in the CNT[76] and between the two parallel plates.[77] Thus, the separation effect could be affected by changing the direction of the electric field.

To determine the electric field effect on the mole fraction in the CNTs, we calculated the axial density distributions of the atoms around the original z axis (Fig. 7). We considered water and methanol molecules in the region from 0 to r_{CNT} (CNT radius), as shown by the dark area in Fig. 7B. As shown in Fig. 7A, for no electric field, the density of methanol molecules near the CNT entrance (vertical black dotted line) is much higher than that in the reservoir region. On the other hand, the density of water molecules is much lower than that in the reservoirs. This is because the van der Waals attraction between the CNT (and graphene) and methanol molecules is stronger than that between the CNT (and graphene) and water molecules.[37] For $\boldsymbol{E}$ = 0.25 V nm^{-1}, the effect of the electric field on the mole fraction in the CNT occurs and χ_{water} increases (Fig. 7B). However, under these conditions, χ_{water} in the CNT is not uniform, where χ_{water} in the right region is higher than that in the left region. As expected, under an electric field, the density of methanol near the right entrance to the CNT is lower than that near the left entrance. On the other hand, the density of water near the right side is higher than that near the left side. That makes χ_{water} in the right region of the CNT higher than that in the left region. Under an electric field, the dipole moments of water and methanol molecules are parallel to the field. The methyl group of methanol is far away from the right graphene sheet but close to the left graphene sheet. Thus, the van der Waals interactions between the right sheet and the methanol molecules are weaker. As a result, the density of methanol molecules near the right sheet is lower than that near the left sheet. This can affect the mole fraction in the CNTs. With the higher electric field of 1 V nm^{-1}, the condition completely changes, where the densities of water molecules near the entrances at both sides are much higher than that in the reservoir region (Fig. 7C). Consequently, only water molecules occupy the CNT.

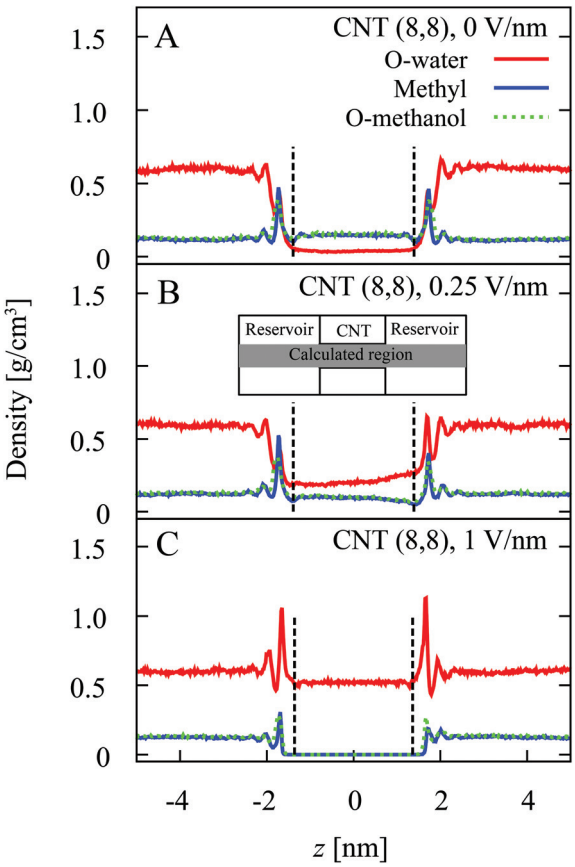

Fig. 7 Axial density distribution of the atoms of water and methanol molecules: (A) E = 0 V nm^{-1}, (B) E = 0.25 V nm^{-1}, and (C) E = 1 V nm^{-1}. The simulation system was a (8, 8) CNT with χ_{water} = 0.81 in the reservoirs. Only the region from 0 to r_{CNT} (CNT radius) from the central axis in the z direction was considered in the calculation, as shown by the dark area. The vertical black dotted lines show the positions of the graphene sheets. O-water and O-methanol denote oxygen atoms of water and methanol, respectively.

4. Conclusions

MD simulations have been performed in a system consisting of a CNT, graphene sheets, and water–methanol reservoirs to investigate the effect of electric fields on the separation of water and methanol molecules. Without an electric field, methanol molecules fill the CNTs in preference to water molecules, resulting in a separation effect for methanol. However, the separation for methanol significantly decreases with increasing CNT diameter. In contrast, under an electric field, water molecules occupy the CNTs in preference to methanol molecules. The preference for water molecules to flow through the CNTs over methanol molecules produces a separation effect for water. Interestingly, the separation effect for water is strong and does not significantly depend on the CNT diameter. The electric field induces the formation of ordered structures of water molecules in the CNTs. This makes the number of hydrogen bonds per molecule for the water molecule structures higher than that for the methanol molecule structures. Consequently, the water molecule structures are stable and methanol molecules are removed from the CNTs. Moreover, methanol molecules from the reservoirs cannot disrupt the water molecule structures and permeate into the CNTs.

Acknowledgements

This work was supported by a Japan Science Promotion Society KAKENHI Grant-in-Aid for Challenging Exploratory Research (grant no. 25630070), a Ministry of Education, Culture, Sports, Science and Technology (MEXT) Grant-in-Aid for the Program for Leading Graduate Schools, the Core Research for Evolutional Science and Technology (CREST) of the Japan Science and Technology Agency, and the Ohtsuki Memorial Scholarship Trust Fund for Asian and African Students.

References

1 G. A. Olah, *Angew. Chem., Int. Ed.*, 2005, **44**, 2636–2639.
2 D. W. Stephan, *Nature*, 2013, **495**, 54–55.
3 M. Nielsen, E. Alberico, W. Baumann, H.-J. Drexler, H. Junge, S. Gladiali and M. Beller, *Nature*, 2013, **495**, 85–89.
4 M. Barinaga, *Nature*, 1987, **327**, 361–361.
5 S. Liu, E. R. Cuty Clemente, T. Hu and Y. Wei, *Appl. Therm. Eng.*, 2007, **27**, 1904–1910.
6 W. Yanju, L. Shenghua, L. Hongsong, Y. Rui, L. Jie and W. Ying, *Energy Fuels*, 2008, **22**, 1254–1259.
7 T. Hu, Y. Wei, S. Liu and L. Zhou, *Energy Fuels*, 2007, **21**, 171–175.
8 B. Höhlein, P. Biedermann, T. Grube and R. Menzer, *J. Power Sources*, 1999, **84**, 203–213.
9 X. Ren, P. Zelenay, S. Thomas, J. Davey and S. Gottesfeld, *J. Power Sources*, 2000, **86**, 111–116.
10 D. A. Boysen, T. Uda, C. R. Chisholm and S. M. Haile, *Science*, 2004, **303**, 68–70.
11 J. Zhang, G.-P. Yin, Q.-Z. Lai, Z.-B. Wang, K.-D. Cai and P. Liu, *J. Power Sources*, 2007, **168**, 453–458.
12 J. Schrader, M. Schilling, D. Holtmann, D. Sell, M. Villela Filho, A. Marx and J. A. Vorholt, *Trends Biotechnol.*, 2009, **27**, 107–115.
13 R. Cortright, R. Davda and J. A. Dumesic, *Nature*, 2002, **418**, 964–967.
14 T. P. Vispute, H. Zhang, A. Sanna, R. Xiao and G. W. Huber, *Science*, 2010, **330**, 1222–1227.
15 J. P. Maity, J. Bundschuh, C.-Y. Chen and P. Bhattacharya, *Energy*, 2014, **78**, 104–113.
16 P. Trop, B. Anicic and D. Goricanec, *Energy*, 2014, **77**, 125–132.
17 Y. Huang, R. W. Baker and L. M. Vane, *Ind. Eng. Chem. Res.*, 2010, **49**, 3760–3768.
18 K. Liang, W. Li, H. Luo, M. Xia and C. Xu, *Ind. Eng. Chem. Res.*, 2014, **53**, 7121–7131.

19 T. C. Bowen, R. D. Noble and J. L. Falconer, *J. Membr. Sci.*, 2004, **245**, 1–33.
20 L. M. Vane, *J. Chem. Technol. Biotechnol.*, 2005, **80**, 603–629.
21 K. Hu, J. Nie, J. Liu and J. Zheng, *J. Appl. Polym. Sci.*, 2013, **128**, 1469–1475.
22 G. Rutkai, É. Csányi and T. Kristóf, *Microporous Mesoporous Mater.*, 2008, **114**, 455–464.
23 T. Remy, J. Cousin Saint Remi, R. Singh, P. A. Webley, G. V. Baron and J. F. Denayer, *J. Phys. Chem. C*, 2011, **115**, 8117–8125.
24 K. Zhang, R. P. Lively, J. D. Noel, M. E. Dose, B. A. McCool, R. R. Chance and W. J. Koros, *Langmuir*, 2012, **28**, 8664–8673.
25 D. Nimcevic and J. R. Gapes, *J. Mol. Microbiol. Biotechnol.*, 2000, **2**, 15–20.
26 A. Chapeaux, L. D. Simoni, T. S. Ronan, M. A. Stadtherr and J. F. Brennecke, *Green Chem.*, 2008, **10**, 1301–1306.
27 L. M. Chávez-Islas, R. Vasquez-Medrano and A. Flores-Tlacuahuac, *Ind. Eng. Chem. Res.*, 2011, **50**, 5153–5168.
28 J. Zang, S. Konduri, S. Nair and D. S. Sholl, *ACS Nano*, 2009, **3**, 1548–1556.
29 G. Arora and S. I. Sandler, *Nano Lett.*, 2007, **7**, 565–569.
30 G. Arora and S. I. Sandler, *J. Chem. Phys.*, 2006, **124**, 084702.
31 W.-F. Chan, H.-y. Chen, A. Surapathi, M. G. Taylor, X. Shao, E. Marand and J. K. Johnson, *ACS Nano*, 2013, **7**, 5308–5319.
32 B. Corry, *Energy Environ. Sci.*, 2011, **4**, 751–759.
33 A. Kalra, S. Garde and G. Hummer, *Proc. Natl. Acad. Sci. U. S. A.*, 2003, **100**, 10175–10180.
34 J. Lee and N. Aluru, *Appl. Phys. Lett.*, 2010, **96**, 133108.
35 O. Sae-Khow and S. Mitra, *J. Phys. Chem. C*, 2010, **114**, 16351–16356.
36 J. Zheng, E. M. Lennon, H.-K. Tsao, Y.-J. Sheng and S. Jiang, *J. Chem. Phys.*, 2005, **122**, 214702.
37 W.-H. Zhao, B. Shang, S.-P. Du, L.-F. Yuan, J. Yang and X. C. Zeng, *J. Chem. Phys.*, 2012, **137**, 034501–034501.
38 X. Tian, Z. Yang, B. Zhou, P. Xiu and Y. Tu, *J. Chem. Phys.*, 2013, **138**, 204711.
39 S. Vaitheeswaran, J. C. Rasaiah and G. Hummer, *J. Chem. Phys.*, 2004, **121**, 7955.
40 F. Mikami, K. Matsuda, H. Kataura and Y. Maniwa, *ACS Nano*, 2009, **3**, 1279–1287.
41 B. Xu, Y. Qiao, Q. Zhou and X. Chen, *Langmuir*, 2011, **27**, 6349–6357.
42 Z. Fu, Y. Luo, J. Ma and G. Wei, *J. Chem. Phys.*, 2011, **134**, 154507.
43 Z. Qian, Z. Fu and G. Wei, *J. Chem. Phys.*, 2014, **140**, 154508.
44 Y. He, G. Sun, K. Koga and L. Xu, *Sci. Rep.*, 2014, **4**, 6596.
45 D. Bratko, C. D. Daub, K. Leung and A. Luzar, *J. Am. Chem. Soc.*, 2007, **129**, 2504–2510.
46 W.-H. Zhao, J. Bai, L.-F. Yuan, J. Yang and X. C. Zeng, *Chem. Sci.*, 2014, **5**, 1757–1764.
47 A. Philippsen, W. Im, A. Engel, T. Schirmer, B. Roux and D. J. Müller, *Biophys. J.*, 2002, **82**, 1667–1676.
48 M. L. Berkowitz, D. L. Bostick and S. Pandit, *Chem. Rev.*, 2006, **106**, 1527–1539.
49 K. F. Rinne, S. Gekle, D. J. Bonthuis and R. R. Netz, *Nano Lett.*, 2012, **12**, 1780–1783.
50 J. Kou, X. Zhou, H. Lu, Y. Xu, F. Wu and J. Fan, *Soft Matter*, 2012, **8**, 12111–12115.
51 S. De Luca, B. Todd, J. Hansen and P. J. Daivis, *J. Chem. Phys.*, 2013, **138**, 154712.
52 S. De Luca, B. D. Todd, J. S. Hansen and P. J. Daivis, *Langmuir*, 2014, **30**, 3095–3109.
53 M. Suk and N. Aluru, *Phys. Chem. Chem. Phys.*, 2009, **11**, 8614–8619.
54 J. Su and H. Guo, *ACS Nano*, 2011, **5**, 351–359.
55 Winarto, D. Takaiwa, E. Yamamoto and K. Yasuoka, *J. Chem. Phys.*, 2015, **142**, 124701.
56 H. Berendsen, J. Postma, W. Van Gunsteren and J. Hermans, *Intermol. Forces*, 1981, **14**, 331–342.
57 W. L. Jorgensen, *J. Phys. Chem.*, 1986, **90**, 1276–1284.
58 W. L. Jorgensen, J. M. Briggs and M. L. Contreras, *J. Phys. Chem.*, 1990, **94**, 1683–1686.
59 A. V. Shevade, S. Jiang and K. E. Gubbins, *J. Chem. Phys.*, 2000, **113**, 6933–6942.
60 A. M. Saitta, F. Saija and P. V. Giaquinta, *Phys. Rev. Lett.*, 2012, **108**, 207801.
61 Y. Zhang, T.-T. Tang, C. Girit, Z. Hao, M. C. Martin, A. Zettl, M. F. Crommie, Y. R. Shen and F. Wang, *Nature*, 2009, **459**, 820–823.
62 B. Hess, C. Kutzner, D. Van Der Spoel and E. Lindahl, *J. Chem. Theory Comput.*, 2008, **4**, 435–447.
63 T. Darden, D. York and L. Pedersen, *J. Chem. Phys.*, 1993, **98**, 10089.
64 J.-P. Ryckaert, G. Ciccotti and H. J. Berendsen, *J. Comput. Phys.*, 1977, **23**, 327–341.
65 S. Nosé, *J. Chem. Phys.*, 1984, **81**, 511.
66 W. G. Hoover, *Phys. Rev. A*, 1985, **31**, 1695.
67 M. Parrinello and A. Rahman, *J. Appl. Phys.*, 1981, **52**, 7182.
68 L. An, J. M. Owens, L. E. McNeil and J. Liu, *J. Am. Chem. Soc.*, 2002, **124**, 13688–13689.
69 A. Okamoto and H. Shinohara, *Carbon*, 2005, **43**, 431–436.
70 T. Thurakitseree, C. Kramberger, A. Kumamoto, S. Chiashi, E. Einarsson and S. Maruyama, *ACS Nano*, 2013, **7**, 2205–2211.
71 M. Ferrario, M. Haughney, I. R. McDonald and M. L. Klein, *J. Chem. Phys.*, 1990, **93**, 5156–5166.
72 M. Pagliai, G. Cardini, R. Righini and V. Schettino, *J. Chem. Phys.*, 2003, **119**, 6655–6662.
73 G. Hummer, J. C. Rasaiah and J. P. Noworyta, *Nature*, 2001, **414**, 188–190.
74 A. Berezhkovskii and G. Hummer, *Phys. Rev. Lett.*, 2002, **89**, 64503.
75 G. Zuo, R. Shen, S. Ma and W. Guo, *ACS Nano*, 2009, **4**, 205–210.
76 L. Figueras and J. Faraudo, *Mol. Simul.*, 2012, **38**, 23–25.
77 H. Qiu and W. Guo, *Phys. Rev. Lett.*, 2013, **110**, 195701.